Cell Reports

Supplemental Information

Loss of BAF (mSWI/SNF) Complexes Causes Global Transcriptional and Chromatin State Changes in Forebrain Development

Ramanathan Narayanan, Mehdi Pirouz, Cemil Kerimoglu, Linh Pham, Robin J. Wagener, Kamila A. Kiszka, Joachim Rosenbusch, Rho H. Seong, Michael Kessel, Andre Fischer, Anastassia Stoykova, Jochen F. Staiger, and Tran Tuoc

SUPPLEMENTAL DATA

Figure S1

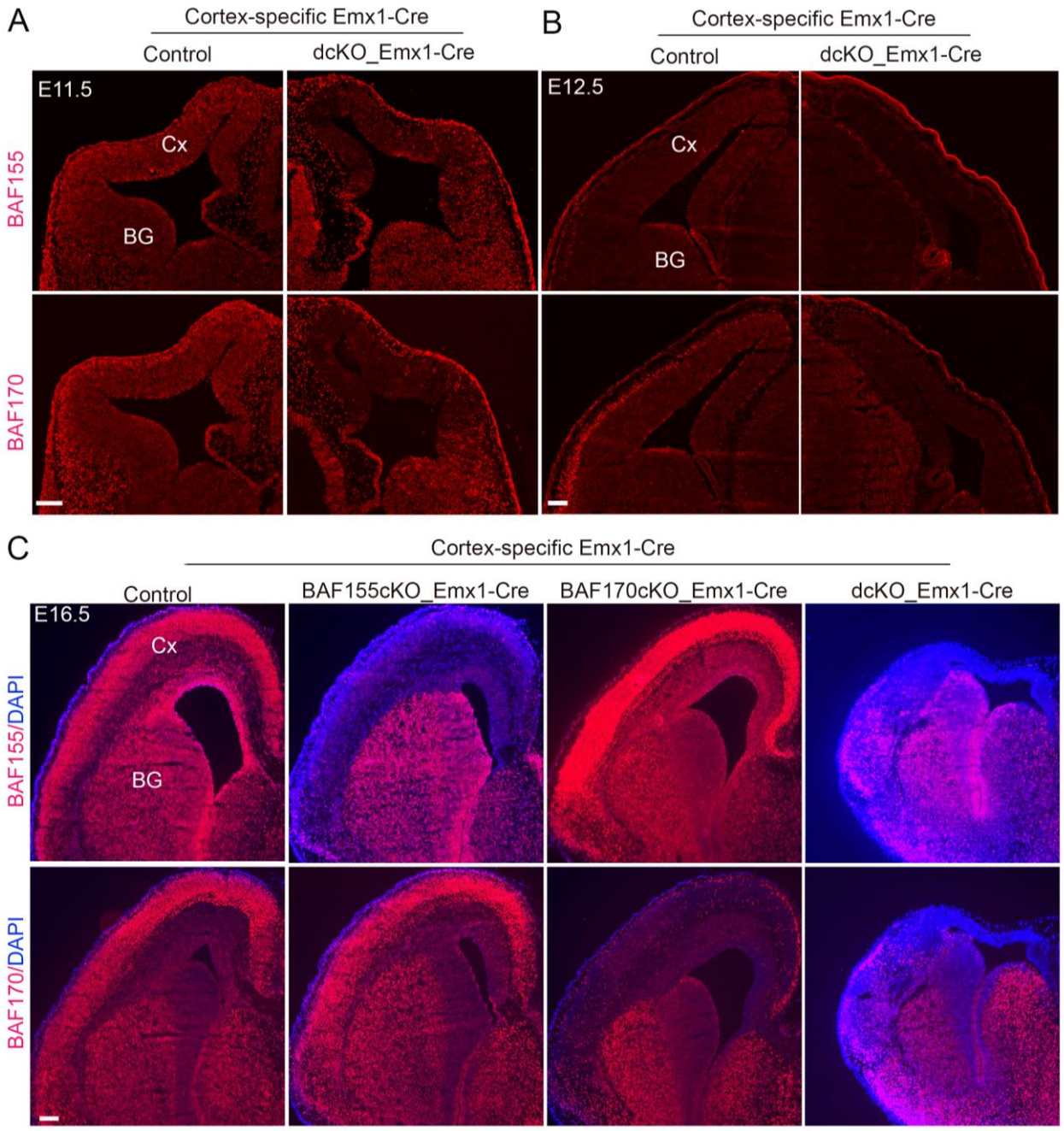

Figure S1 (related to figure 1). Expression of BAF155 and BAF170 in mutant cortices.

(A–C) IHC analysis of E11.5 (A), E12.5 (B), and E16.5 (C) cortical coronal sections with BAF155 and BAF170 antibodies showing residual expression of BAF155 and BAF170 at E11.5 (A), and a complete loss at E12.5 and E16.5 (B-C) in dcKO_*Emx1*-Cre mutants. Note that the dcKO_*Emx1*-Cre mutant has a much thinner cortex than the control at E16.5. In addition, BAF170 ablation in *BAF170*cKO_*Emx1*-Cre cortex leads to highly increased expression of BAF155, whereas expression of BAF170 in the cortex is not different in *BAF155*cKO_*Emx1*-Cre and control embryos (B). Abbreviations: Cx, cortex; BG, basal ganglion. Scale bars = 150 μm (A and B) and 100 μm (C).

Figure S2

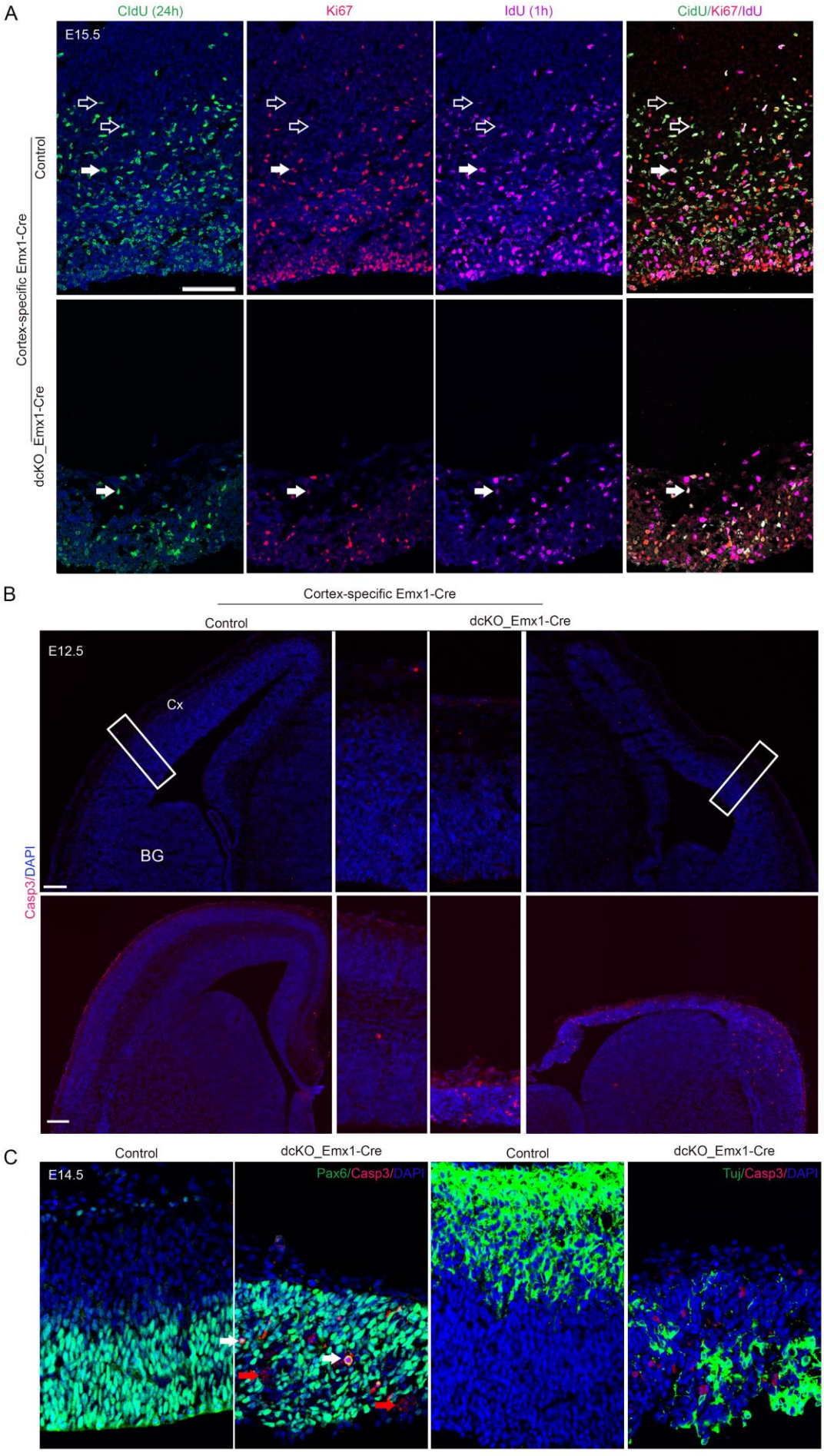
A
CldU (24h)
Ki67
IdU (1h)
CidU/Ki67/IdU
E15.5
Control
Cortex-specific Emx1-Cre
dcKO_Emx1-Cre
B
Cortex-specific Emx1-Cre
Control
dcKO_Emx1-Cre
E12.5
Cx
BG
Casp3/DAPI
C
Control
dcKO_Emx1-Cre
Control
dcKO_Emx1-Cre
E14.5
Pax6/Casp3/DAPI
Tuj/Casp3/DAPI

Figure S2 (related to figure 2). Corticogenesis in dcKO mutants.

(A) Images show triple-label IHC of cortical sections with antibodies for CidU (24-h labeling; marks both exited and cycling progenitors), IdU (1-h labeling; a marker for S-phase progenitors), and Ki67 (a marker for proliferating progenitors, except those in late G2 phase) at E15.5 (see Fig. 2D/E for experimental paradigm and statistical analysis). (B) IHC shows that cortical tissues of dcKO-*Emx1*_Cre embryos have a low number of Casp3+ apoptotic cells at E12.5 and a high number at E15.5 (see Fig. 1F for quantitative analyses). The middle panels are higher-magnification images from the fields in the cortex indicated by white frames. (C) Double IHC analyses of Pax6/Casp3 and Tuj/Casp3 show that most Casp3+ cells are either immunoreactive for Pax6 (white arrows) or with punctate forms (at the late phase of apoptosis, red arrows) (see also Fig. 2F for quantitative analyses). Values are presented as means ± SEMs (n = 6; ***$P < 0.005$; NS, not significant.) Abbreviations: Cx, cortex; BG, basal ganglion. Scale bars = 100 μm.

Figure S3

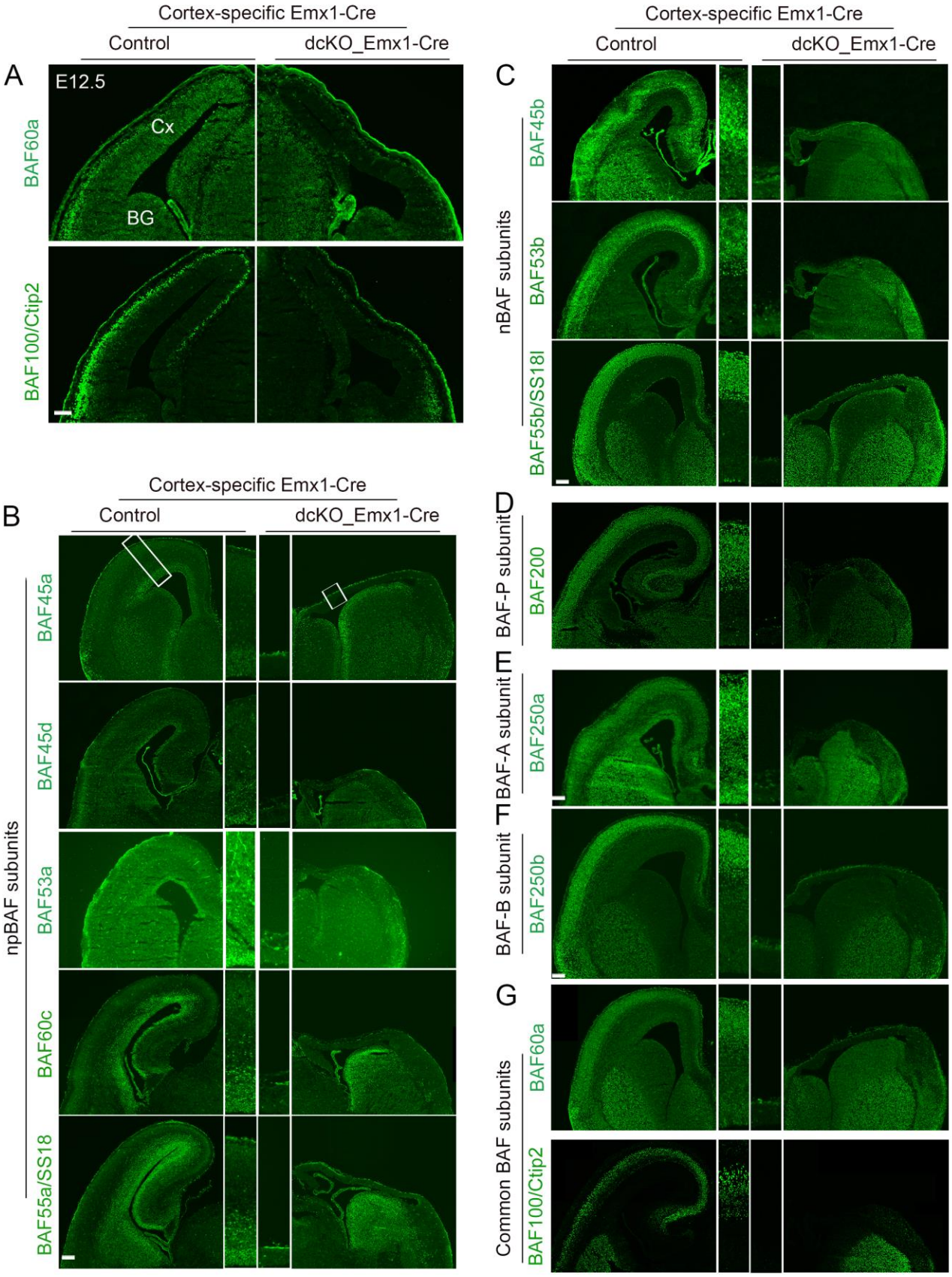
A
Cortex-specific Emx1-Cre
Control
dcKO_Emx1-Cre
E12.5
Cx
BG
BAF60a
BAF100/Ctip2
B
Cortex-specific Emx1-Cre
Control
dcKO_Emx1-Cre
npBAF subunits
BAF45a
BAF45d
BAF53a
BAF60c
BAF55a/SS18
C
Cortex-specific Emx1-Cre
Control
dcKO_Emx1-Cre
nBAF subunits
BAF45b
BAF53b
BAF55b/SS18l
D
BAF-P subunit
BAF200
E
BAF-A subunit
BAF250a
F
BAF-B subunit
BAF250b
G
Common BAF subunits
BAF60a
BAF100/Ctip2

Figure S3 (related to figure 3). Expression of BAF subunits in dcKO mutants in vivo. (A–G) Images show IHC analyses for subunits of BAF complexes (Lessard et al., 2007; Wang et al., 1996; Yan et al., 2008) in cortical tissue from cortex-specific dcKO_*Emx1*-Cre embryos and controls at E12.5 (A) and E16.5 (B–G), including those that are unique for the npBAF complex in neural progenitors (BAF45a/d, BAF53a, BAF60c, SS18) (B), the nBAF complex in neurons (BAF45b, BAF53b, SS18l) (C), the polybromo-associated (P) BAF complex (BAF200) (D), the BAF-A complex (BAF250a) (E) and the BAF-B complex (BAF250b) (F), and subunits that are common to many BAF complexes (Brg1, Brm, BAF60a, BAF47, Ctip2) (G and Fig. 2A). Our data indicate that expression of all BAF subunits is largely absent in BAF155/BAF170-deficient cortices. Abbreviation: Cx, cortex; BG, basal ganglion. Scale bars = 150 μm (A) and 100 μm (B–G).

Figure S4

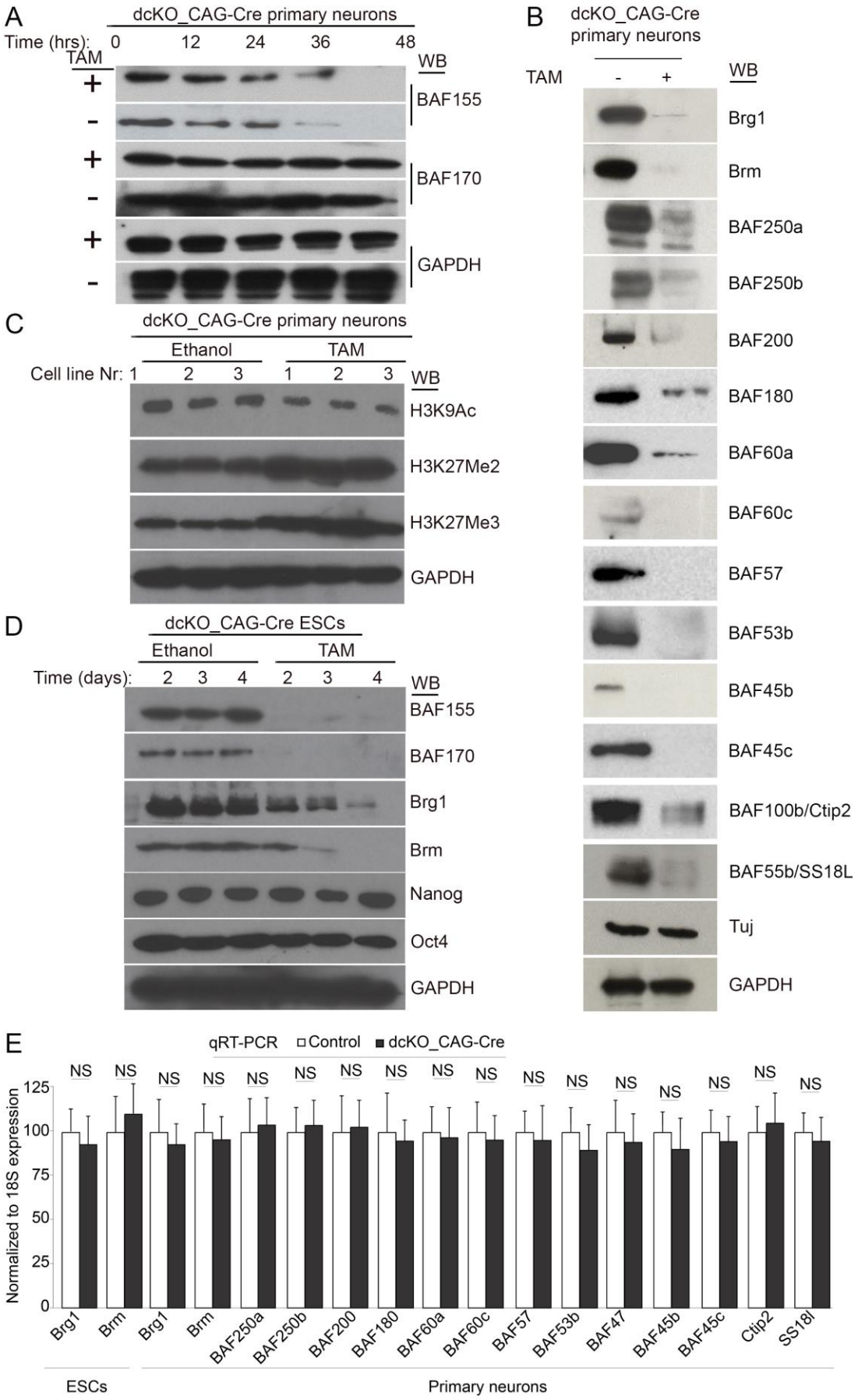
A
dcKO_CAG-Cre primary neurons
Time (hrs): 0 12 24 36 48
TAM
WB
BAF155
BAF170
GAPDH
B
dcKO_CAG-Cre primary neurons
TAM - +
WB
Brg1
Brm
BAF250a
BAF250b
BAF200
BAF180
BAF60a
BAF60c
BAF57
BAF53b
BAF45b
BAF45c
BAF100b/Ctip2
BAF55b/SS18L
Tuj
GAPDH
C
dcKO_CAG-Cre primary neurons
Ethanol
TAM
Cell line Nr: 1 2 3 1 2 3
WB
H3K9Ac
H3K27Me2
H3K27Me3
GAPDH
D
dcKO_CAG-Cre ESCs
Ethanol
TAM
Time (days): 2 3 4 2 3 4
WB
BAF155
BAF170
Brg1
Brm
Nanog
Oct4
GAPDH
E
qRT-PCR
Control
dcKO_CAG-Cre
Normalized to 18S expression
125
100
75
50
25
0
NS
Brg1
Brm
Brg1
Brm
BAF250a
BAF250b
BAF200
BAF180
BAF60a
BAF60c
BAF57
BAF53b
BAF47
BAF45b
BAF45c
Ctip2
SS18l
ESCs
Primary neurons

Figure S4 (related to figure 3). Expression of BAF subunits and level of H3K27Me2/3 in dcKO primary neurons and embryonic stem cells. (A) WB analyses showing an absence of BAF155 and BAF170 proteins in dcKO_*CAG*-Cre primary neurons after 2 d of TAM treatment. (B) WB analyses showing a near-complete loss of all known nBAF subunits in dcKO_*CAG*-Cre primary neurons after 5 d of TAM treatment. (C) Augmented H3K27Me2/3 levels in dcKO_*CAG*-Cre primary neurons after 5 d of TAM treatment compared with ethanol-treated control cells. (D) BAF155 and BAF170 depletion did not cause a loss of pluripotency marker expression, but almost eliminated esBAF subunits as shown for Brm and Brg1 protein in dcKO_*CAG*-Cre ESCs after 2–4 days of TAM treatment. (E) qRT-PCR analyses of transcripts for BAF subunits in dcKO_*CAG*-Cre primary neurons (in B) compared with controls. Values are presented as means ± SEMs (n = 6; NS, not significant).

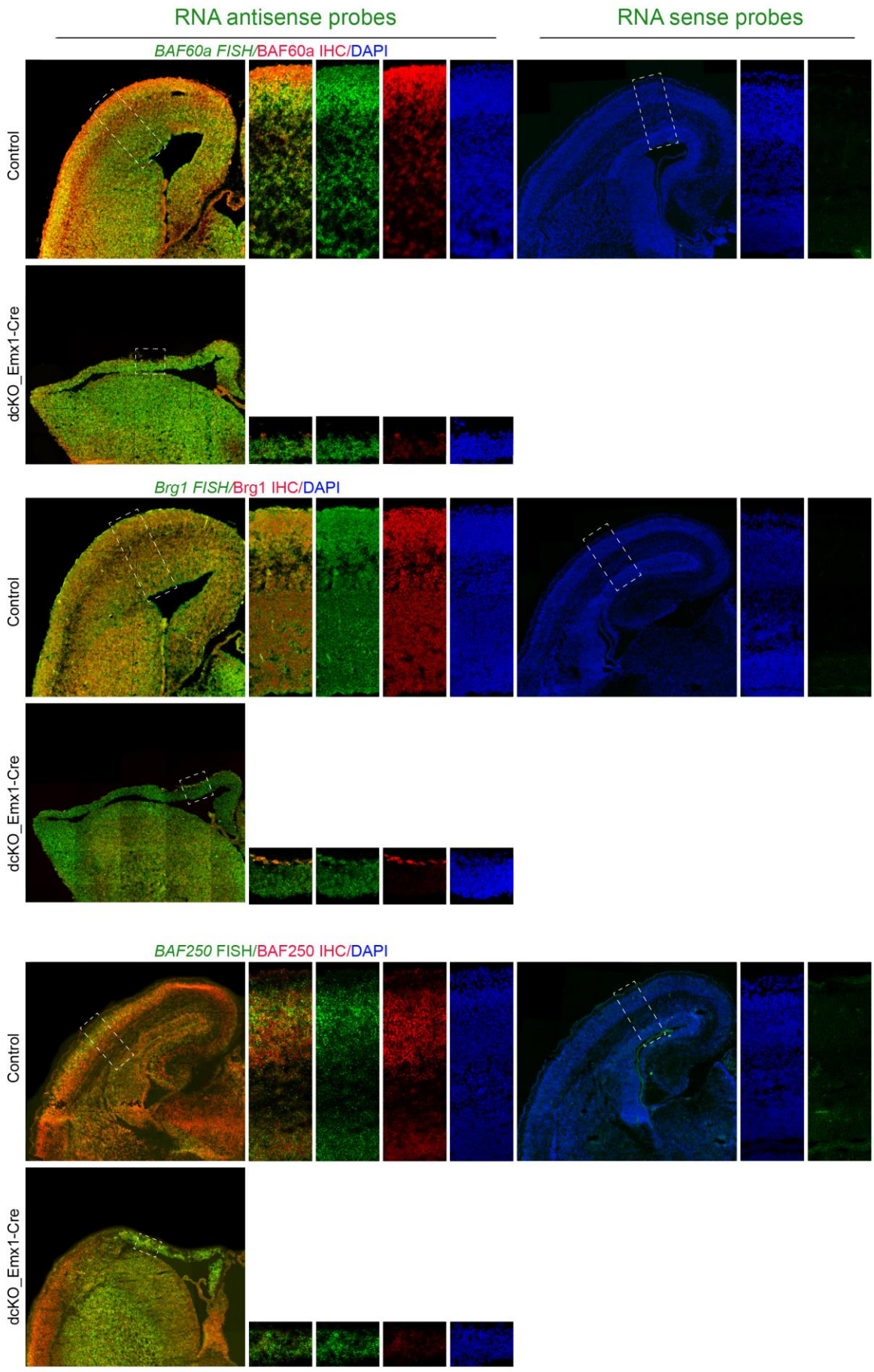
RNA antisense probes
RNA sense probes
BAF60a FISH/BAF60a IHC/DAPI
Control
dcKO_Emx1-Cre
Brg1 FISH/Brg1 IHC/DAPI
Control
dcKO_Emx1-Cre
BAF250 FISH/BAF250 IHC/DAPI
Control
dcKO_Emx1-Cre

Figure S5 (related to figure 3). Examination of the expression of BAF subunits in double FISH/IHC.

Combined FISH, with RNA sense and antisense probes (green), and IHC (red) analyses of Brg1, BAF60a and BAF260a transcripts and proteins in the cortex of dcKO_*Emx1*-Cre mutants at E16.5. The absence of a green signal in FISH with RNA sense probes (image on right) suggests specificity of the generated sense probes for Brg1, BAF60a, and BAF260a transcripts (images on left; green). Note loss of proteins (green), but not transcripts, of Brg1, BAF60a, and BAF260a in the dcKO_*Emx1*-Cre cortex. Scale bar = 100 μm.

Figure S6

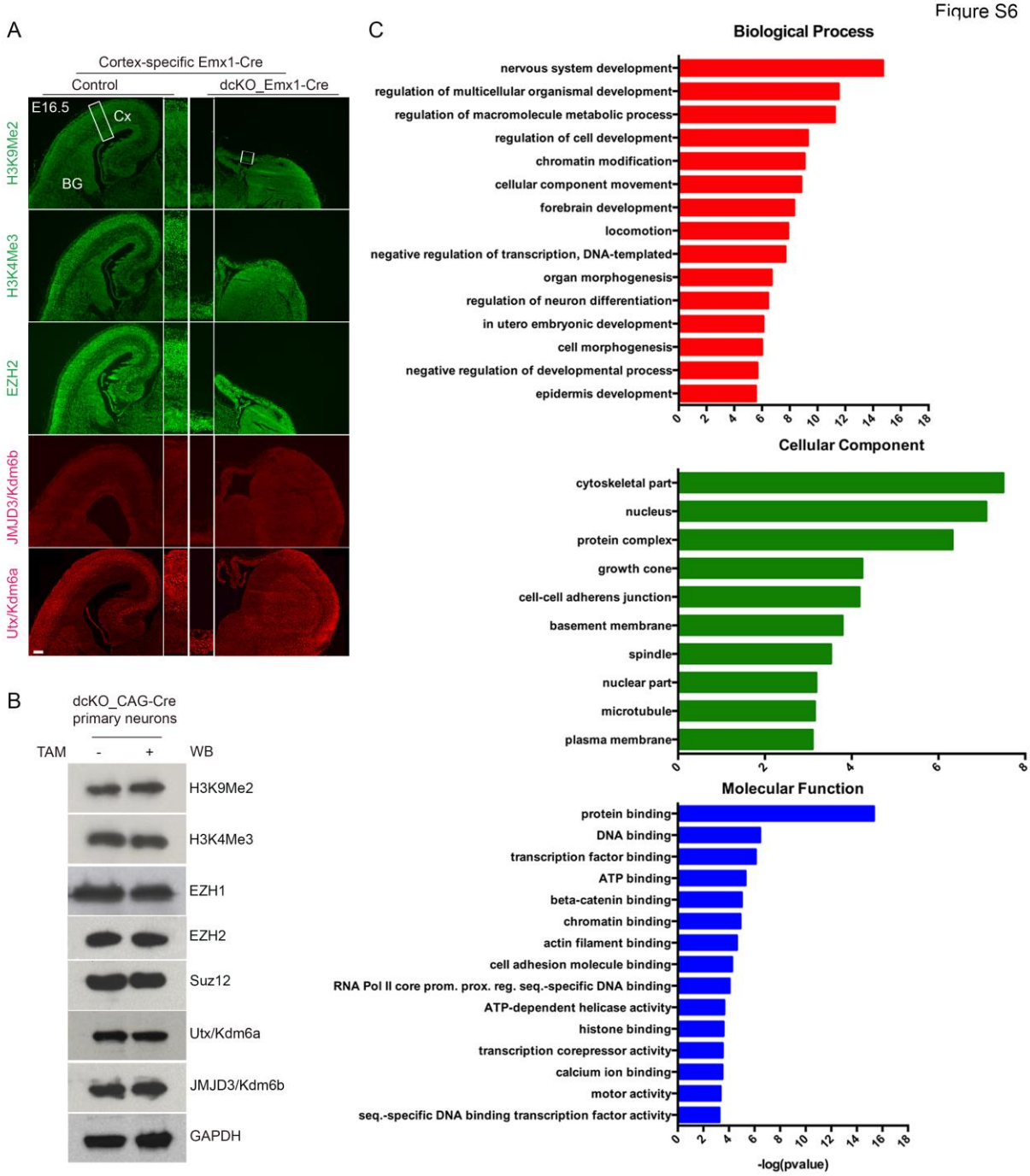
A
Cortex-specific Emx1-Cre
Control
dcKO_Emx1-Cre
E16.5
Cx
BG
H3K9Me2
H3K4Me3
EZH2
JMJD3/Kdm6b
Utx/Kdm6a
B
dcKO_CAG-Cre
primary neurons
TAM
-
+
WB
H3K9Me2
H3K4Me3
EZH1
EZH2
Suz12
Utx/Kdm6a
JMJD3/Kdm6b
GAPDH
C
Biological Process
nervous system development
regulation of multicellular organismal development
regulation of macromolecule metabolic process
regulation of cell development
chromatin modification
cellular component movement
forebrain development
locomotion
negative regulation of transcription, DNA-templated
organ morphogenesis
regulation of neuron differentiation
in utero embryonic development
cell morphogenesis
negative regulation of developmental process
epidermis development
0 2 4 6 8 10 12 14 16 18
Cellular Component
cytoskeletal part
nucleus
protein complex
growth cone
cell-cell adherens junction
basement membrane
spindle
nuclear part
microtubule
plasma membrane
0 2 4 6 8
Molecular Function
protein binding
DNA binding
transcription factor binding
ATP binding
beta-catenin binding
chromatin binding
actin filament binding
cell adhesion molecule binding
RNA Pol II core prom. prox. reg. seq.-specific DNA binding
ATP-dependent helicase activity
histone binding
transcription corepressor activity
calcium ion binding
motor activity
seq.-specific DNA binding transcription factor activity
0 2 4 6 8 10 12 14 16 18
-log(pvalue)

Figure S6 (related to figure 5 and 6). H3 levels, expression of H3K27Me2/3-modifying enzymes in dcKO mutants and Gene Ontology (GO) analysis. (A and B) Expression of other modified H3 forms (H3K9Me2, H3K4Me3) (A), and H3K27 methytransferases (EZH1, EZH2, Suz12) and H3K27 demethylases (UTX/Kdm6a, JMJD3/Kdm6b) (B) is preserved in cortices of cortex-specific dcKO-*Emx1*_Cre and dcKO-*CAG*_Cre primary neurons compared with controls. Scale bars = 100 μm. (C) GO categories enriched in the set of genes whose expression was significantly changed in the dcKO_*Emx1*-Cre cortex at E12.5, classified into subcategories of the three main GO sub-groups: biological process, cellular component, and molecular function. These categories were selected by comparison with the complete set of genes represented by the microarray using the hypergeometric test in the FUNC package (Prufer et al., 2007).

A

Protein	Accession	Number of peptides					
		BAF155 coIP/MS			BAF170 coIP/MS		
		cortical NSCs	E13.5 forebrains	E17.5 forebrains	cortical NSCs	E13.5 forebrains	E17.5 forebrains
Kdm6a/Utx	gi|33859492	6	13	9	7	5	19
Kdm6b/JMJD3	gi|148678553	12	10	5	7	8	15

B

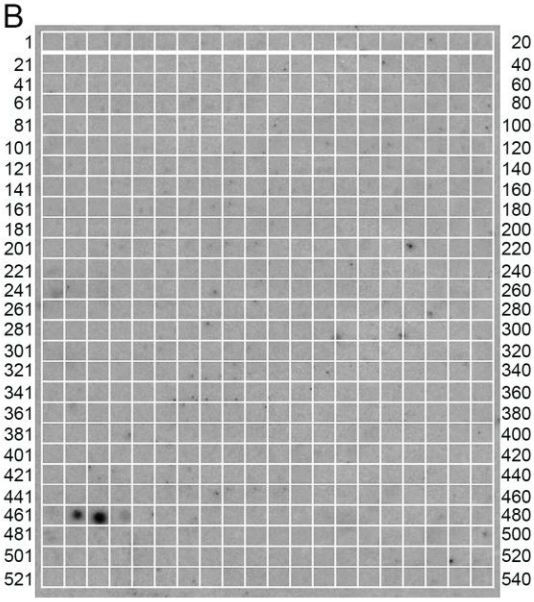

C

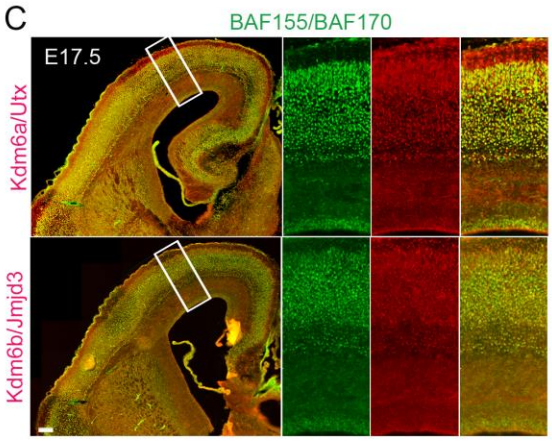

Figure S7 (related to figure 7). BAF155 and BAF170 interact with H3K27 demethylases. (A) Table showing the number of peptides for UTX/Kdm6a and JMJD3/Kdm6b proteins purified by BAF155 or BAF170-immunoprecipitation (BAF155 CoIP/MS or BAF170 CoIP/MS) of crude protein extracts from NS5 cells, or E13.5 or E17.5 forebrain tissues. (B) Fully developed film of a peptide array for a purified Flag-tagged BAF155 and BAF170 protein mixture and spotted Kdm6b/Jmjd3 peptides (see also Fig. 4B). (C) Double-label IHC analysis with anti-BAF155/BAF170 antibodies (green) and anti-UTX/Kdm6a or anti-JMJD3/Kdm6b antibodies (red), showing co-expression of BAF155/BAF170 with UTX/Kdm6a and JMJD3/Kdm6b in forebrain cells. Scale bars = 100 μm.

- **Table S1 (related to figure 6A).** Genes Regulated by BAF155 and BAF170 in the Developing dcKO_*Emx1*-Cre Cortex at E12.5 (As a Supplemental Spreadsheet).
- **Table S2 (related to figure 6A, 6B, S6C):** Selected Gene Ontology Categories Significantly Enriched in E12.5 dcKO_*Emx1*-Cre Embryos Compared with Controls in Expression Analyses (As a Supplemental Spreadsheet).
- **Table S3 (related to figure 2C/E/F, 5B)**: statistical analyses

SUPPLEMENTAL EXPERIMENTAL PROCEDURES

Plasmids

Plasmids used in this study: JMJD3-HA (De Santa et al., 2007), Utx-HA (Agger et al., 2007), BAF47-Flag (Sohn et al., 2007), BAF155-Flag (Sohn et al., 2007), BAF170-Flag (Xi et al., 2008) from Addgene, Brm-Flag (Sif et al., 2001) from Addgene, Brg-Flag (Sohn et al., 2007).

Antibodies

The following polyclonal (pAb) and monoclonal (mAb) primary antibodies used in this study were obtained from the indicated commercial sources: Brg1 rabbit pAb (Santa Cruz), Brg1 mouse mAb (Santa Cruz), Brm mouse mAb (BD Biosciences), Brm rabbit pAb (Abcam), BAF250 mouse mAb (Sigma), BAF180 rabbit pAb (Bethyl), BAF170 rabbit pAb (Bethyl), BAF170 rabbit pAb (Sigma), BAF155 rabbit pAb (Santa Cruz), BAF155 mouse mAb (Santa Cruz), BAF60a mouse mAb (BD Biosciences), BAF60c mouse mAb (Abnova), BAF57 rabbit pAb (Bethyl), BAF45b rabbit pAb (Abcam), BAF45d rabbit pAb (Santa Cruz), BAF47 rabbit pAb (Abcam), Ctip1 mouse mAb

(Abcam), Ctip2 rat pAb (1:200; Abcam), SS18 rabbit pAb (Abcam), SS18l/Crest goat pAb (Santa Cruz), GAPDH rabbit pAb (Santa Cruz), ß-actin rabbit pAb (Sigma), H3K9Ac rabbit pAb (Abcam), H3K27me2 rabbit pAb (Cell Signaling), H3K27me3 rabbit pAb (Upstate), H3 rabbit pAb (Upstate), Kdm6a/Utx rabbit pAb (Santa Cruz), Kdm6b/jmjd3 rabbit pAb (De Santa et al., 2007), Ezh1 rabbit pAb (1:1000; Abcam), Cux1 rabbit pAb (1:100; Santa Cruz), Satb2 mouse mAb (1:100; Abcam), Casp-3 rabbit pAb (1:100; Cell Signaling), Sox2 mouse mAb (R&D Systems), Pax6 mAb (Developmental Studies Hybridoma Bank), Pax6 rabbit pAb (BABCO), Flag mAb (1:1000; Sigma), phospho-H3 mAb (1:50; Cell Signaling), Tuj mAb (1:200; Chemicon), Tbr2 rabbit pAb (1:300; Chemicon), RORc mouse mAb (1:100; Perseus Proteomics), and Tle1 rabbit pAb (1:200; Abcam). Secondary antibodies used were peroxidase-conjugated goat anti-rabbit IgG (1:10000; Covance); peroxidase-conjugated goat anti-mouse IgG (1:5000; Covance); peroxidase-conjugated goat anti-rat IgG (1:10000; Covance); and Alexa 488-, Alexa 568-, Alexa 594- and Alexa 647-conjugated IgG (various species,1:400; Molecular Probes). BAF53a, BAF53b BAF45a and BAF45c rabbit pAbs were kindly provided by Dr. Crabtree (Stanford University), and the Ngn2 mouse mAb was a gift from Dr. Anderson (California Institute of Technology).

Generation of dcKO mutants

To eliminate *BAF155* and *BAF170* in the entire telencephalon, in the cortex or in projection neurons, we used the corresponding Cre mouse lines, forebrain-specific *FoxG1*-Cre (Hebert and McConnell, 2000), cortex-specific *Emx1-Cre* (Gorski et al., 2002) and neuron-specific *Nex*-Cre (Goebbels et al., 2006). Heterozygous animals (*BAF155*$^{fl/+}$, *BAF170*$^{fl/+}$, *Cre*) were used as controls. Mutants crossed with *FoxG1*-Cre, *Emx1*-Cre, or *Nex*-Cre died soon after birth.

To generate full dcKO_*CAG*-Cre mutants, we used the ubiquitous, inducible *CAG-Cre* mouse line (Hayashi and McMahon, 2002). Homozygous mice (BAF155$^{fl/fl}$, BAF170$^{fl/fl}$, *Cre*) treated with vehicle were used as controls. dcKO_*CAG*-Cre mutants treated with TAM at E10.5 died between E14.5 and E15.5 with severe developmental retardation.

Derivation and culture of mouse embryonic stem cells

Mouse embryonic stem cells (ESCs) were generated by triple crosses of Esr-Cre, BAF155$^{fl/fl}$, and BAF170$^{fl/fl}$ mice. Blastocysts were individually plated on gelatin-coated 24-well culture dishes (day 0). Blastocysts were cultured in N2B27 medium supplemented with LIF and the GSK3 and MAP kinase inhibitors CHIR 99021 (3 μM) and PD 0325901 (1 μM), respectively, as previously described (Ying et al., 2008).

During the first 3 d of culture, dishes were left completely undisturbed to avoid detachment of blastocysts. The medium was changed on day 3. The following day (day 4), cells were trypsinized using 100 µl ES-trypsin, and a single-cell suspension was prepared by pipetting up and down with a 2-ml pipette. The trypsin was neutralized by adding 1 ml of medium, and then suspensions were plated in individual wells of a 4-well culture dish. The first colonies emerged on day 6 or 7 (passage #1 [P1]); cultures were numbered based on the order of ESC colony appearance. On day 9, cultures were washed with phosphate-buffered saline (PBS), trypsinized with 175 µl ES-trypsin, neutralized with 1 ml medium, and then plated on gelatin-coated 12-well plates containing 1 ml ES medium (P2). Upon reaching confluence, cultures were either frozen or split into new dishes and fed fresh medium every other day. Pure ESCs were used for DNA extraction and genotyping.

Chromatin immunoprecipitation

All steps were carried out in DNA low-binding tubes from Diagenode (DNA LoBind). Mouse embryonic cortices were homogenized in sucrose solution (0.32 M sucrose, 5 mM $CaCl_2$, 5 mM $Mg(Ac)_2$, 0.1 mM EDTA, 50 mM HEPES pH 8, 1 mM DTT, 0.1% Triton X-100), fixed in 37% formaldehyde, and then treated with 1.25 M glycine. The samples were then centrifuged, and the pellet (i.e., nuclei) was washed with Nelson buffer (140 mM NaCl, 20 mM EDTA pH 8, 50 mM Tris pH 8, 0.5% NP-40, 1% Triton X-100). Thereafter, nuclei were re-suspended in RIPA-SDS buffer (140 mM NaCl, 1 mM EDTA, 1% Triton X-100, 0.1% sodium deoxycholate, 10 mM Tris pH 8, 1% SDS) and incubated on a rotating wheel for 10 min at 4°C. The samples were then transferred to sonication tubes (Diagenode) and sonicated in a Bioruptor Plus NGS (Diagenode) at a setting of “High” at 4°C. Samples were spun down after every fifth cycle to ensure homogeneous shearing. After sonication, samples were centrifuged at 18,000 × g for 5 min and the supernatant was transferred to a fresh tube. The sheared chromatin was snap frozen and kept at -80°C prior to any further treatment. A small amount was kept in order to test shearing efficiency and total chromatin amount using an Agilent 2100 Bioanalyzer (Agilent Technologies) and QuBit fluorometer (Life Technologies), respectively, after reverse-crosslinking. To that end, samples were treated with 0.1 µg/µl RNase A (Qiagen) and Proteinase K (Roth).

Protein A-coated Dynabeads (Life Technologies) were blocked by incubating 40 µl of beads with 500 µl of 0.5% bovine serum albumen (BSA) for 2 h at 4°C on a rotating wheel. The chromatin was diluted 10-fold in immunoprecipitation (IP) buffer (140 mM NaCl, 1% NP-40, 0.5% sodium deoxycholate, 50 mM Tris pH 8, 20 mM EDTA, 0.1% SDS) and pre-cleared by incubating with 20 µl of blocked beads for 1 h

at 4°C on a rotating wheel. For immunoprecipitation, 1000 ng of pre-cleared chromatin was incubated overnight at 4°C on a rotating wheel with 2 µg of anti-H3K27me3 antibody (Millipore). The next day, the samples were incubated with 15 µl of coated beads for 2 h at 4°C on a rotating wheel. Beads were then washed with IP buffer and wash buffer (100 mM Tris pH 8, 500 mM LiCl, 1% NP-40, 1% sodium deoxycholate, 20 mM EDTA), and collected on magnetic stands (Invitrogen). DNA was eluted with 20 µl elution buffer (10 mM Tris pH 8) containing 0.1 µg/µl RNase A. Samples were incubated for 30 min at 37°C in a thermomixer (Eppendorf) with gentle agitation, then diluted 2-fold with Wiemann Buffer (100 mM Tris pH 8, 20 mM EDTA, 2% SDS) containing 1 µl of Proteinase K (20 µg/µl) and incubated overnight at 65°C in a thermomixer (Eppendorf) with agitation. The next day, 3 µl of linear polyacrylamide (Bioline) and 60 µl of SureClean (Bioline) were added to the samples. Samples were then transferred to magnetic stands, the beads were washed with 70% ethanol, and DNA was eluted with 30 µl elution buffer. Inputs were handled in parallel with immunoprecipitated samples. Finally, DNA quality and quantity were measured on an Agilent 2100 Bioanalyzer and QuBit fluorometer, respectively.

ChIP-Seq

7 libraries were prepared from E13.5 cortices of *dcKO_Emx1*-Cre embryos (Control: n=4, *dcKO*: n=3) and 7 libraries from P1 cortices of *dcKO_Nex*-Cre mice (Control: n=4, *dcKO*: n=3). All library preparations were done according to the Illumina standard protocol (TruSeq; Illumina). Input DNA was isolated from all the samples and was pooled for each group above separately. Thus additionally 4 input libraries (1 for each group) were sequenced. The quality and quantity of the libraries were measured with an Agilent 2100 Bioanalyzer and QuBit fluorometer, respectively.

Base calling and conversion to fastq format were performed using Illumina pipeline scripts. Afterwards, quality control on raw data was conducted for each library (FastQC, www.bioinformatics.babraham.ac.uk/projects/fastqc). The following control measurements and information were obtained: per base sequence quality, per sequence quality scores, per base sequence content, per base GC content, per sequence GC content, per base N content, sequence length distribution, sequence duplication levels, overrepresented sequences, Kmer content.

The reads were mapped to a mouse reference genome (mm10) using STAR aligner v2.3.0 (Djebali et al., 2012). *rmdup* and *merge* functions of samtools (Li et al., 2009) were used to remove PCR duplicates from each BAM file and for merging replicates from the same groups into a single BAM file respectively. Downstream

analyses were performed on the merged BAM files from immunoprecipitated samples and inputs. Profile plots of H3K27me3 were created with NGSPlot using non-default parameters (Shen et al., 2014). Paired student t-test was performed on the data used for generating the plots. H3K27me3 binding on and around different gene loci was visualized through the Integrated Genome Browser (Nicol et al., 2009) using wiggle files that were created from the merged BAM files with the script from the MEDIPS package of Bioconductor (Lienhard et al., 2014).

Co-immunoprecipitation and Mass spectrometry (coIP/MS)

BAF155 and BAF170 interaction analyses were performed using neural stem cells (NS5) (Conti et al., 2005) and E13.5 and E17.5 embryonic telecephalic tissue. Tissues were dissected and minced in cold PBS and then washed twice with PBS. Equivalent cells from one embryo were lysed for 30 min in 1 ml RIPA buffer containing a proteinase inhibitor cocktail (Roche) and DNAse. All steps were performed at 4°C. Lysates were centrifuged for 10 min at 13,000 rpm to exclude non-lysed tissues. The supernatant was pre-cleared by incubating with normal mouse IgG together with protein A/G-agarose beads as described by the manufacturer (sc-2003; Santa Cruz). Pre-cleared supernatant was incubated with rabbit anti-BAF155 and anti-BAF170 antibodies and A/G-agarose beads to immunoprecipitate interacting proteins. The beads were then washed first with 500 µl cold RIPA buffer (three times for 5 min each) and then with 40 µl elution buffer (2.5 µl 20% SDS, 5 µl 1 M $NaHCO_3$ and 42.5 µl double-distilled H_2O) for 15 min at room temperature.

Samples were suspended in NuPage loading buffer and resolved on commercial SDS gels (Novex NuPage Bis-Tris gel, 4–12% gradient; Invitrogen) in the department of Prof. Dr. Henning Urlaub. Individual lanes were then cut into six squares for MS analysis. The parameters for the identification of proteins were set to the following values: limit, 95% probability of detection; limit of unique peptides detected, 1; and threshold detection probability of peptides, 80%.

The list of BAF155 and BAF170-interacting proteins in mass spectrometry analysis was obtained by subtracting unspecific interactions in IPs with IgG and with tissues from BAF155 and BAF170 null mutants. First, with IgG negative controls, we excluded the unspecific bindings to the antibody. Second, we performed IP using anti-BAF155 and and anti-BAF170 with telencephalic tissue of *BAF155cKO_FoxG1*-Cre and *BAF170cKO_FoxG1*-Cre mutants as well. This excludes unspecific interactions

that possibly could be precipitated by any of the anti-BAF155 or anti-BAF170 antibodies.

Protein-protein interaction assay

CoIP analysis and Flag IP were performed as described previously (Tuoc and Stoykova, 2008a). To block the interaction between BAF170 and JMJD3/UTX, purified BAF155/BAF170 proteins was pre-incubated with the synthesized peptide 462-463 (peptide sequence: RTPGHQENNNFCSVNINIGPGDC) of JMJD3 (Figure 7B).

Peptide array affinity assay

Customized Kdm6b/Jmjd3 peptide arrays were obtained from JPT Peptide Technologies. Peptides with acetylated N-termini were synthesized and covalently bound through their C-termini with a polyethylene glycol linker to the cellulose membrane (5 nmol/spot). The mixture of purified Flag-BAF155 and Flag-BAF170 was analyzed on affinity arrays using the manufacturer's protocol. Briefly, the peptide array was blocked with 0.3% low-fat milk in 1X Tris-buffered saline (TBS/0.3% milk) for 1 h and subsequently incubated with 5 µg/ml of the protein mixture (in 50 mM Tris/HCl pH 7.0, 150 mM NaCl) overnight at 4°C. Protein–peptide binding was detected by incubating first with rabbit anti-Flag primary antibody (1:1000 in TBS/0.3% milk) for 3 h and then with HRP-conjugated anti-mouse secondary antibody (1:5000 in TBS/0.3% milk) for 1 h. The membrane was washed three times (10 min each) with TBS/0.3% milk after incubations with primary and secondary antibodies. Immunoreactive proteins were detected using ECL Plus detection reagents. Next, the membrane was stripped and incubated with purified Flag to confirm no interaction between Flag and peptides.

Standard and cortical primary cell cultures

Cortical primary cells were dissociated from mouse embryos and cultured as described previously (Conti et al., 2005; Tuoc and Stoykova, 2008a). For cell culture assays, plasmids were transfected into Neuro2A cells using Lipofectamine 2000, or were electroporated into primary cortical cells using a mouse neural cell Nucleofector kit and a nucleotransfection device (Amaxa).

4-Hydroxytamoxifen treatment

4-Hydroxytamoxifen (TAM) (H6278, Sigma) was19dissolved19in ethanol to a final stock concentration of 10 mM (10,000x). Cultured cells were treated with 1 µM TAM or ethanol (vehicle control). During treatment, media were replaced with fresh media containing 1 µM TAM or ethanol every 48 h.

Treatment with GSK-126 in vivo.

For in vivo treatment, the histone methyltransferase EZH2 inhibitor GSK126 (A-1275; Active Biochem) was dissolved in DMSO. Pregnant dcKO_*Emx1*-Cre mice at E11.5 and E12.5 were injected intraperitoneally with DMSO (vehicle) or with GSK126 at a dose of 50–150 mg/kg body weight (McCabe et al., 2012; Sato et al., 2013).

Cycloheximide pulse-chase protein stability assay

Protein stability was assessed using a cycloheximide pulse-chase protocol in the presence or absence of the proteasome inhibitor MG132, as described previously (Tuoc and Stoykova, 2008a). Briefly, 18 h after treatment with TAM, dcKO_*CAG*-Cre primary neurons were cultured with the protein biosynthesis inhibitor cyclohexamide, with or without MG-132, and protein levels were assessed by WB analysis.

Complex stability assay

dcKO_*CAG*-Cre primary neurons were treated with or without TAM for 48 h and subsequently incubated with the proteasome inhibitor MG132 for an additional 30 h. For CoIP experiments, nuclear extracts were immunoprecipitated with antibodies against Brg1 and Brm, and then probed with antibodies against BAF subunits by WB analysis.

In vitro and in vivo demethylase assays

In vitro demethylase assays were performed as described (Jepsen et al., 2007; Tsukada et al., 2006). Briefly, a reconstituted BAF complex (recBAF) (Phelan et al., 1999) containing five core subunits (Brg1, Brm, BAF155, BAF170, and BAF47), together with either purified Flag-Jmjd3 or purified Flag-Utx, was incubated with calf thymus histones (Sigma) at 37°C for 1–3 h in histone demethylation buffer (50 mM HEPES-KOH pH 7.5, 70 mM $Fe(NH_4)_2(SO_4)_2$, 1 mM α-ketoglutarate, and 2 mM ascorbate). For *in vivo* demethylase assays, cultured dcKO_CAG-Cre neurons were nucleofected with a mammalian expression vector for either UTX/Kdm6a-ires-GFP or JMJD3/Kdm6b ires-GFP. Recombination of BAF155 and BAF170 alleles was induced by adding TAM to the growth medium at a final concentration of 1 µM. After 2 DIV, GFP+ cells were enriched by FACS and harvested for WB analysis. The demethylase activities of UTX/Kdm6a and JMJD3/Kdm6b were determined by measuring histone methylation levels by Western blotting using antibodies against H3K27me2 and H3K27me3.

Fluorescent in situ hybridization (FISH)

Digoxigenin (DIG)-labeled cRNA probes were generated from the appropriate plasmids containing full-length or partial cDNA inserts specific for the respective BAF subunits (NCBI Gene IDs: BAF250b/Arid1b, 239985; BAF60a/Smarcd1, 83797; Brg1/Smarca4, 20586). After restriction digestion with the appropriate enzymes and subsequent in vitro transcription using a DIG RNA labeling kit (Roche), the size of probes was reduced to 350 base pairs by alkaline hydrolysis (0.2 M sodium carbonate and 0.2 M sodium bicarbonate at pH 10.2). Frozen, fixed brain sections (12-µm thick) on slides were post-fixed with 4% paraformaldehyde (PFA; 3 min at 4°C) and rinsed two times (3 min each) with 0.01 M PBS. Endogenous peroxidase signals were quenched with 1% H_2O_2 (15 min) followed by rinsing, treatment with 0.2 M HCl, additional rinsing, and digestion with proteinase K (20 µg/ml; 3 min). After repeating PFA fixation, the tissue was treated with 0.1 M triethanolamine/HCl and acetic anhydride (10 min), rinsed, and treated with an ascending alcohol series. Tissue sections were prehybridized by incubating in hybridization buffer (HB; 50% formamide, 4x SSC, 250 µg/ml denatured salmon sperm DNA, 100 µg/ml tRNA, 5% dextran sulfate and 1% Denhardt's solution) for 1 h at 55°C. Hybridization was performed by incubating overnight at 55°C with DIG-labeled probes (200 ng/ml). Post-hybridization wash steps were performed at 65°C, starting with 5x standard saline citrate (SSC) for 1 min, then followed by 2x SSC/50% formamide for 30 min, 1x SSC/50% formamide for 30 min, and 0.1x SSC for 30 min (1x SSC: 0.15 M NaCl, 0.015 M sodium citrate, pH 7.0). After blocking twice (10 min each) with 5% sheep serum and 0.5% blocking buffer (Perkin Elmer) in 0.01 M TBS (pH 7.4) at room temperature, probes were detected by incubating overnight at 4°C with peroxidase-conjugated anti-DIG Fab fragments (raised in sheep serum; Roche), diluted 1:2000 in TBS containing blocking agent. The signal was amplified using biotinyl tyramide signal amplification, according to the manufacturer's protocol (TSA Plus Biotin System; Perkin Elmer). Probes were visualized using Alexa 488-coupled streptavidin (Life Technologies).

IHC and cell-cycle parameter experiments

IHC and determination of cell-cycle index were performed as previously described (Tuoc et al., 2009).

qRT-PCR and WB analyses

qRT-PCR and WB analyses were performed as described previously (Tuoc and Stoykova, 2008a) using primers described in Supplementary Table 2 and the Mouse Neurogenesis RT² Profiler PCR Array profiles (Qiagen).

mRNA expression profiling and data analysis

Detailed protocols of RNA purification and data analysis were described previously (Tuoc et al., 2013). Briefly, RNA was extracted from both hemispheres from three control and three dcKO E12.5 littermate mice using an RNAeasy kit (Qiagen).

The RNA quality assessment was provided as part of the gene expression service (Cambridge Genomic Services). The three quality criteria are concentration, purity and integrity. The concentration and purity of RNA were measured and evaluated by using UV absorption with a spectrophotometer plate reader, the SpectroStar (BMG Labtech). RNA has their absorption maximum at 260 nm and the ratio of the absorbance at 260 and 280 nm is used to assess the purity of an RNA preparation. Pure RNAs have an A260/A280 of 1.8 to 2.1. The RNA integrity is assessed on the Agilent 2100 Bioanalyzer, which generates a RIN number (RNA Integrity Number). Total RNA run on the Agilent 2100 Bioanalyzer shows two distinct ribosomal peaks corresponding to 18S and 28S for eukaryotic RNA and a relatively flat baseline between the 5S and 18S ribosomal peaks. For all microarray analyses, RIN must be higher than 8. Only RNA samples, which passed the quality assessment, are processed further.

Gene expression in each sample was assayed using Illumina Mouse WG6 v2.0 BeadChip microarrays. Probes passing a detection p-value threshold of 0.01 were selected using the R package lumi (Du et al., 2008). The data were then transformed using variance stabilisation (Lin et al., 2008) and quantile normalised before the identification of significant changes in gene expression (eBayes, Benjamini-Hochberg corrected p-value < 0.05) using Limma (Smyth, 2005). According to the QC report generated using the arrayQualityMetrics R package (Illumina), no samples failed or are outliers to their replicates.

Genes showing significant changes in expression in the dcKO_*Emx1*-Cre were compared to genes previously identified as Ezh2-regulated in the E12.5 *Ezh2*cKO_*Emx1-Cre* neocortex (Pereira et al., 2010). Before the comparison all microarray probes were re-annotated to the latest MGI gene symbols using ProbeLynx (http://koch.pathogenomics.ca/probelynx/, (Roche et al., 2004), and genes not common to both microarray platforms were removed from the analysis.

Gene Ontology categories for down-regulated genes in the E12.5 cortex of dcKO_*Emx1*-Cre mice were identified using hypergeometric tests in the FUNC package (Prufer et al., 2007)

Image acquisition and statistical analysis

All images were acquired with standard (Leica DM 6000) and confocal (Leica TCS SP5) fluorescence microscopes, or an Axio Imager M2 (Zeiss) with a Neurolucida system (MBF Bioscience). Images were further analyzed with Adobe Photoshop. Statistical analyses were done using Student's t-test. All bar graphs are plotted as means ± SEM.

Quantitative analysis of immunohistochemical signal intensity

For the quantitative analyses of immunohistochemical signal intensity of H3K9Ac and H3K27Me2/3 (Figure 5A/B), fluorescent images of sections of telencephalons were used. The IHC Images with corresponding IgG isotopes were used as immune-staining controls. The color images of forebrains were converted to gray scale to eliminate background. The pixel values of the fluorescent signal intensity were measured by using Analyze/Analyze Particles function (ImageJ software) as previously described (Tuoc et al., 2013; Tuoc and Stoykova, 2008a). The measured value was then subtracted from immune-staining controls (without primary antibody). In the cortex-specific dcKO_*Emx1*-Cre, we measured signal intensity in the cortex (where expression of BAF155/BAF170 is lost in mutants) and in the basal ganglion (unaltered expression of BAF155/BAF170 in mutants) as internal control. Compared to the control at E14.5-E16.5, the ventricular zone (VZ), intermediate zone (IZ) and cortical plate (CP) of the cortex in dcKO_*Emx1*-Cre mutants was thinner and disorganized, therefore we quantified the signal intensity of entire cortex as a single field. In the control cortex, a mean from measurement of three fields (VZ, IZ, CP) was used.

Similarly the relative amount of protein from developed films in WB experiment was quantified densitometrically using ImageJ software as described previously (Tuoc and Stoykova, 2008b).

SUPPLEMENTAL REFERENCES

Agger, K., Cloos, P.A., Christensen, J., Pasini, D., Rose, S., Rappsilber, J., Issaeva, I., Canaani, E., Salcini, A.E., and Helin, K. (2007). UTX and JMJD3 are histone H3K27 demethylases involved in HOX gene regulation and development. Nature *449*, 731-734.

Conti, L., Pollard, S.M., Gorba, T., Reitano, E., Toselli, M., Biella, G., Sun, Y., Sanzone, S., Ying, Q.L., Cattaneo, E*., et al.* (2005). Niche-independent symmetrical self-renewal of a mammalian tissue stem cell. PLoS Biol *3*, e283.

De Santa, F., Totaro, M.G., Prosperini, E., Notarbartolo, S., Testa, G., and Natoli, G. (2007). The histone H3 lysine-27 demethylase Jmjd3 links inflammation to inhibition of polycomb-mediated gene silencing. Cell *130*, 1083-1094.

Djebali, S., Davis, C.A., Merkel, A., Dobin, A., Lassmann, T., Mortazavi, A., Tanzer, A., Lagarde, J., Lin, W., Schlesinger, F*., et al.* (2012). Landscape of transcription in human cells. Nature *489*, 101-108.

Du, P., Kibbe, W.A., and Lin, S.M. (2008). lumi: a pipeline for processing Illumina microarray. Bioinformatics *24*, 1547-1548.

Goebbels, S., Bormuth, I., Bode, U., Hermanson, O., Schwab, M.H., and Nave, K.A. (2006). Genetic targeting of principal neurons in neocortex and hippocampus of NEX-Cre mice. Genesis *44*, 611-621.

Gorski, J.A., Talley, T., Qiu, M., Puelles, L., Rubenstein, J.L., and Jones, K.R. (2002). Cortical excitatory neurons and glia, but not GABAergic neurons, are produced in the Emx1-expressing lineage. J Neurosci *22*, 6309-6314.

Hayashi, S., and McMahon, A.P. (2002). Efficient recombination in diverse tissues by a tamoxifen-inducible form of Cre: a tool for temporally regulated gene activation/inactivation in the mouse. Dev Biol *244*, 305-318.

Hebert, J.M., and McConnell, S.K. (2000). Targeting of cre to the Foxg1 (BF-1) locus mediates loxP recombination in the telencephalon and other developing head structures. Dev Biol *222*, 296-306.

Jepsen, K., Solum, D., Zhou, T., McEvilly, R.J., Kim, H.J., Glass, C.K., Hermanson, O., and Rosenfeld, M.G. (2007). SMRT-mediated repression of an H3K27 demethylase in progression from neural stem cell to neuron. Nature *450*, 415-419.

Lessard, J., Wu, J.I., Ranish, J.A., Wan, M., Winslow, M.M., Staahl, B.T., Wu, H., Aebersold, R., Graef, I.A., and Crabtree, G.R. (2007). An essential switch in subunit composition of a chromatin remodeling complex during neural development. Neuron *55*, 201-215.

Li, H., Handsaker, B., Wysoker, A., Fennell, T., Ruan, J., Homer, N., Marth, G., Abecasis, G., Durbin, R., and Genome Project Data Processing, S. (2009). The Sequence Alignment/Map format and SAMtools. Bioinformatics *25*, 2078-2079.

Lienhard, M., Grimm, C., Morkel, M., Herwig, R., and Chavez, L. (2014). MEDIPS: genome-wide differential coverage analysis of sequencing data derived from DNA enrichment experiments. Bioinformatics *30*, 284-286.

Lin, S.M., Du, P., Huber, W., and Kibbe, W.A. (2008). Model-based variance-stabilizing transformation for Illumina microarray data. Nucleic acids research *36*, e11.

McCabe, M.T., Ott, H.M., Ganji, G., Korenchuk, S., Thompson, C., Van Aller, G.S., Liu, Y., Graves, A.P., Della Pietra, A., 3rd, Diaz, E*., et al.* (2012). EZH2 inhibition as a therapeutic strategy for lymphoma with EZH2-activating mutations. Nature *492*, 108-112.

Nicol, J.W., Helt, G.A., Blanchard, S.G., Jr., Raja, A., and Loraine, A.E. (2009). The Integrated Genome Browser: free software for distribution and exploration of genome-scale datasets. Bioinformatics *25*, 2730-2731.

Pereira, J.D., Sansom, S.N., Smith, J., Dobenecker, M.W., Tarakhovsky, A., and Livesey, F.J. (2010). Ezh2, the histone methyltransferase of PRC2, regulates the balance between self-renewal and differentiation in the cerebral cortex. Proceedings of the National Academy of Sciences of the United States of America *107*, 15957-15962.

Phelan, M.L., Sif, S., Narlikar, G.J., and Kingston, R.E. (1999). Reconstitution of a core chromatin remodeling complex from SWI/SNF subunits. Molecular cell *3*, 247-253.

Prufer, K., Muetzel, B., Do, H.H., Weiss, G., Khaitovich, P., Rahm, E., Paabo, S., Lachmann, M., and Enard, W. (2007). FUNC: a package for detecting significant associations between gene sets and ontological annotations. BMC Bioinformatics *8*, 41.

Roche, F.M., Hokamp, K., Acab, M., Babiuk, L.A., Hancock, R.E., and Brinkman, F.S. (2004). ProbeLynx: a tool for updating the association of microarray probes to genes. Nucleic acids research *32*, W471-474.

Sato, T., Kaneda, A., Tsuji, S., Isagawa, T., Yamamoto, S., Fujita, T., Yamanaka, R., Tanaka, Y., Nukiwa, T., Marquez, V.E., *et al.* (2013). PRC2 overexpression and PRC2-target gene repression relating to poorer prognosis in small cell lung cancer. Sci Rep *3*, 1911.
Shen, L., Shao, N., Liu, X., and Nestler, E. (2014). ngs.plot: Quick mining and visualization of next-generation sequencing data by integrating genomic databases. BMC genomics *15*, 284.
Sif, S., Saurin, A.J., Imbalzano, A.N., and Kingston, R.E. (2001). Purification and characterization of mSin3A-containing Brg1 and hBrm chromatin remodeling complexes. Genes & development *15*, 603-618.
Smyth, G. (2005). Limma: Linear models for microarray data. Bioinformatics and Computational Biology Solutions using R and Bioconductor. Springer, New York, 397–420.
Sohn, D.H., Lee, K.Y., Lee, C., Oh, J., Chung, H., Jeon, S.H., and Seong, R.H. (2007). SRG3 interacts directly with the major components of the SWI/SNF chromatin remodeling complex and protects them from proteasomal degradation. J Biol Chem *282*, 10614-10624.
Tsukada, Y., Fang, J., Erdjument-Bromage, H., Warren, M.E., Borchers, C.H., Tempst, P., and Zhang, Y. (2006). Histone demethylation by a family of JmjC domain-containing proteins. Nature *439*, 811-816.
Tuoc, T.C., Boretius, S., Sansom, S.N., Pitulescu, M.E., Frahm, J., Livesey, F.J., and Stoykova, A. (2013). Chromatin regulation by BAF170 controls cerebral cortical size and thickness. Developmental Cell *25*, 256-269.
Tuoc, T.C., Radyushkin, K., Tonchev, A.B., Pinon, M.C., Ashery-Padan, R., Molnar, Z., Davidoff, M.S., and Stoykova, A. (2009). Selective cortical layering abnormalities and behavioral deficits in cortex-specific Pax6 knock-out mice. The Journal of neuroscience : the official journal of the Society for Neuroscience *29*, 8335-8349.
Tuoc, T.C., and Stoykova, A. (2008a). Trim11 modulates the function of neurogenic transcription factor Pax6 through ubiquitin-proteosome system. Genes Dev *22*, 1972-1986.
Tuoc, T.C., and Stoykova, A. (2008b). Trim11 modulates the function of neurogenic transcription factor Pax6 through ubiquitin-proteosome system. Genes & development *22*, 1972-1986.
Wang, W., Cote, J., Xue, Y., Zhou, S., Khavari, P.A., Biggar, S.R., Muchardt, C., Kalpana, G.V., Goff, S.P., Yaniv, M., *et al.* (1996). Purification and biochemical heterogeneity of the mammalian SWI-SNF complex. The EMBO journal *15*, 5370-5382.
Xi, Q., He, W., Zhang, X.H., Le, H.V., and Massague, J. (2008). Genome-wide impact of the BRG1 SWI/SNF chromatin remodeler on the transforming growth factor beta transcriptional program. The Journal of biological chemistry *283*, 1146-1155.
Yan, Z., Wang, Z., Sharova, L., Sharov, A.A., Ling, C., Piao, Y., Aiba, K., Matoba, R., Wang, W., and Ko, M.S. (2008). BAF250B-associated SWI/SNF chromatin-remodeling complex is required to maintain undifferentiated mouse embryonic stem cells. Stem Cells *26*, 1155-1165.
Ying, Q.L., Wray, J., Nichols, J., Batlle-Morera, L., Doble, B., Woodgett, J., Cohen, P., and Smith, A. (2008). The ground state of embryonic stem cell self-renewal. Nature *453*, 519-523.